2010 NDIA GROUND VEHICLE SYSTEMS ENGINEERING AND TECHNOLOGY SYMPOSIUM
MODELING & SIMULATION, TESTING AND VALIDATION (MSTV) MINI-SYMPOSIUM
AUGUST 17-19 DEARBORN, MICHIGAN

Durability Analysis for Off-Road Vehicle Stowage Systems

Nammalwar Purushothaman, PhD
James Critchley, PhD
Jessica Hulings
U.S. Combat Systems
BAE Systems
Troy, MI

Amarendra Joshi
Altair Engineering
Troy, MI

ABSTRACT

Durability analysis as applied to high mobility off-road ground vehicles involves simulating the vehicle on rough terrains and cascading the loads throughout the structure to support the verification of various components. For components within the hull structure, the rigid body accelerations of the hull are transformed to the component location producing a prescribed g-load time history. This modeling method works extremely well for items which are bolted in place but is inappropriate for stowage systems such as boxes and shelves where cargo can experience intermittent contact and impacts. One solution is to create a dynamic contact nonlinear finite element model of the stowage solution with supported cargo and subject them to the same acceleration profile. This approach effectively resolves the stresses needed to perform fatigue evaluations but is a computationally and labor intensive process. The resources required for single design point verification cannot be justified for simple stowage elements, not to mention the possibility of design iteration. To address the need for rapid assessment of stowage systems, a simplified model is presented then tuned and validated relative to the finite element contact model. This model uses a set of particles to represent the stowed component and interacts with the stowage surface through an effective stiffness, allowing it to be thrown free of the surface and collide generating increased loads. All three approaches (transformed g-loads, FE contact, and particle approximation) are demonstrated with loose cargo in a stowage box. The three models demonstrate similar performance for mild excitations and more vigorous inputs result in larger loads from the two contact models. The load profiles generated by the particle approximation are demonstrated to be consistent with the variability of the overall durability process, justifying their use as an independent predictive tool.

INTRODUCTION

Vehicle durability refers to the long term performance of a vehicle under the repetitive loading due to driving and other operating conditions. In normal operating conditions, tires and suspensions experience road loads which cascade throughout the vehicle body. The transfer and distribution of loads varies with the structural, inertial, and material attributes of the vehicle body and manifest as repetitive loads on the system and components. These repetitive loads cause fatigue damage and the accumulation of damage ultimately results in the initiation of cracks, crack propagation, and system or part failure. A design for durability process is a method of managing the accumulation of fatigue damage to prevent cracks from initiating in advance of the complete design life of the vehicle.

The high level approaches to the design of durable automotive systems have been classified as (i) design-build-test-fix; (ii) design-prototype-measure-analyze; and (iii) virtual test. The commercial automotive industry applies method (ii) with success. This is attributed to the idea that that new vehicles are similar in weight, geometry, suspension characteristics, and operational capability with existing models. The risk of a significant durability issue is effectively mitigated by design experience and large volumes of relevant test data. In this case the process effectively identifies all issues as minor fixes which are readily applied to production ready designs.

In contrast to the commercial automotive process, it is common for each military ground vehicle program to define a new weight class, geometry, suspension, and operational capability. When applying durability design methods

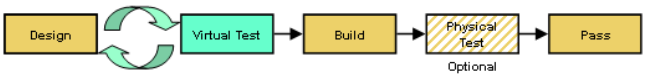

Figure 1: The virtual test durability process.

described by (ii) the risk of the initial design defects is significant. Following this process can require the construction of many costly vehicle prototypes before a design is ready for build. The virtual test durability process shown in Figure 1 eliminates the need for multiple vehicle builds [1].

The analysis of ancillary vehicle components which are bolted or welded in place is performed by cascading the vehicle hull accelerations to the component and generating local time histories corresponding to the duty cycle. Having been obtained for repetitive durability events rather than one time strength events, a passable design will have sprung mass (chassis or hull) g-loads which are sufficiently limited to allow quasi-static linear analysis. Resonances can be captured via direct linear transient simulation or ignored if all modes exceed the suspension wheel hop frequency.

From this perspective, stowage systems present a unique challenge as the cargo is not generally constrained to move with the supporting surface. Furthermore the military off-road duty cycle routinely exceeds gravity in the vertical direction which can throw objects and create the potential for larger impact loads.

The following sections introduce an example stowage system consisting of design, test, and virtual verification. Virtual verification is then demonstrated using the common restrained mass approach and a dynamic explicit FEA solution. The shortcomings of each are discussed and a reduced order model capable of capturing the essential features is formulated, presented, configured, and validated. Conclusions are presented summarizing the simulation time and durability prediction performance of the new model.

AN EXAMPLE SYSTEM

In this section a representative stowage problem is given as a box located on the exterior of a vehicle. The required physical testing conditions are then described and translated into the necessary components of a virtual durability modeling procedure.

Stowage Solution Design

The stowage box as shown in Figure 2 is a light weight (39 kg) sheet steel (2.0 mm thick Steel-UML_UTS300) box measuring 1.6 x 0.5 x 0.6 meters. The box is to be rated for a 91 kg capacity (200 lbs) and bolted to the hull at four locations. The bolts are positioned symmetrically about the center of back plate 0.6 meters side to side and 0.2 meters

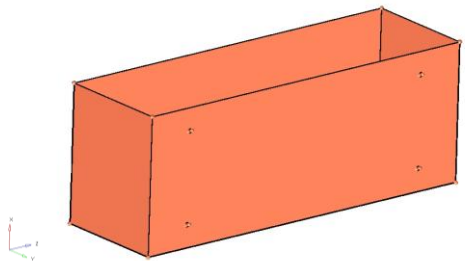

Figure 2: The stowage box design.

vertically. With respect to the vehicle, the box is attached 2 meters to the rear, 1.25 meters to the right side, and 1.25 meters up from the vehicle center of mass. The vehicle to which the stowage solution is mounted is a heavy armored off road truck with thick plates forming the hull which are appropriately considered as a rigid attachment for lighter weight components.

Testing Environment

For physical test the stowage box will be loaded with an equivalent fabric bag filled with sand to 91 kg. The sand is dry regular and of type fine washed or similar. The sand has a density of approximately 1600 kg/m^3 and occupies a volume of roughly 5x10^{-2} cubic meters.

The loaded vehicle will be driven over primary roads for 4500 miles periodically entering a standard 5 mile durability course at 21 mph to accumulate an additional 500 miles. The box will be inspected at the conclusion of testing and is said to pass if there are no visible signs of damage (cracks).

Predictive Virtual Evaluation

The virtual durability process consists of five activities as shown in process flow of Figure 3. The activities are duty cycle development, computation of vehicle dynamic behavior and extraction of loads, pseudo damage evaluation, structural modeling, and fatigue life evaluation. It is

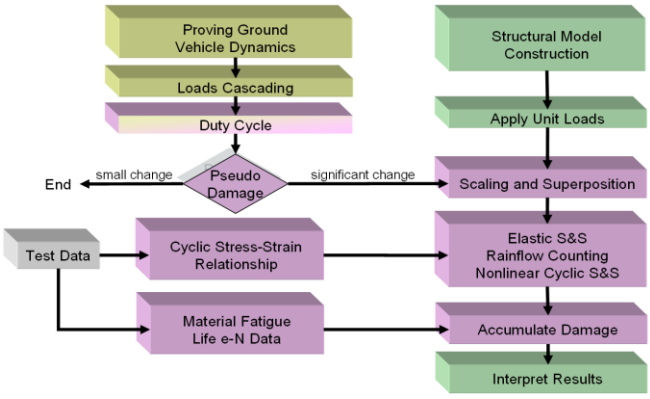

Figure 3: Durability process summary.

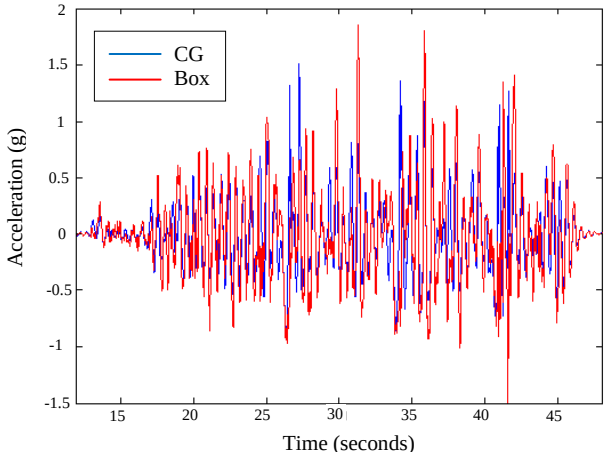

Figure 4: Chassis/hull vertical accelerations.

important to note that the simulation of strength events (those events which are expected to cause immediate and perceptible damage) is also an important aspect of durability. Simulations of such discrete events are commonplace in today's analysis environment and will not be discussed further. From this point on, the terms fatigue and durability will be used interchangeably in reference to the virtual durability process.

The duty cycle approximates the 5000 miles of test by ignoring the smooth primary road inputs and focusing on the durability segment. The durability segment is 5 miles long and represents over 14 minutes of driving time. It is common to select a representative subset of the terrain because generating road loads from simulated vehicle dynamics is time and resource intensive. In this case a 300 meter segment will be used which is repeated 2,682 times to accumulate 500 miles. This assumption can be validated using historical data and reference predictions. For the purposes of this example validation is assumed.

The effect of the stowage system on the gross vehicle dynamics is negligible such that the heavy vehicle can be driven in simulation independently over the rough terrain. A full complement of rigid body time histories has been recorded and saved from a DADS vehicle model on terrain. For the 300 meter section of track at 21 mph the trajectory of the rigid hull has been identified by six degree of freedom motions of the hull center of mass and reference frame. The vertical acceleration of the center of mass is shown in Figure 4. All six components of the chassis motion participate in the transformation to the accelerations at the attachment point with the vertical component also shown in Figure 4.

An un-calibrated relative damage can be obtained immediately using only the g-loads (accelerations multiplied by mass). This pseudo damage is computed using the strain life curve, rain-flow counting, and Miner's rule. In addition to providing quick estimates of changes in duty cycle criteria, this calculation is also very useful when considering changes in mounting location or reuse of the same stowage element in alternate locations. Upon completion of a single iteration of durability prediction, the pseudo damage can be correlated to the predicted damage values to rapidly identify changes in performance due to adjustments in ride (the chassis accelerations).

The g-loads may be applied to the structural analysis in a generic manner. Supported models may be quasi-static or modal transient (restrained mass assumption for cargo), dynamic contact with implicit or explicit FEA solvers (free cargo), or any other solution method which provides stress and strain time histories over the simulated event. The details of three specific approaches are discussed in later sections.

Given a resultant stress or strain time history, the fatigue software nCode Design Life [2] is then used to estimate the damage of the box due to the virtual duty cycle approximation. The nCode software material database provides material fatigue properties for Steel-UML_UTS300 which is shown in Figures 5 through 7. The standard rain-flow cycle counting process is applied and damage is accumulated on individual elements of the FEA model. Damage in excess of 1.0 corresponds to the initiation of cracks within the duty cycle which are assumed to propagate quickly (to visible failure).

Significant sources of variability are present in the analysis environment and the hardware design and test. It is therefore important to consider the effect of variability in the predicted fatigue life. A discussion of variability applied to similar vehicle components and testing can be found in [1].

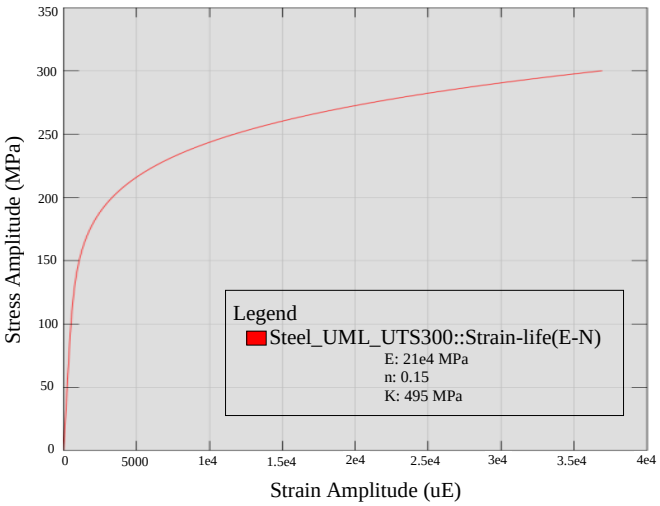

Figure 5: Cyclic stress-strain (Steel UML UTS300).

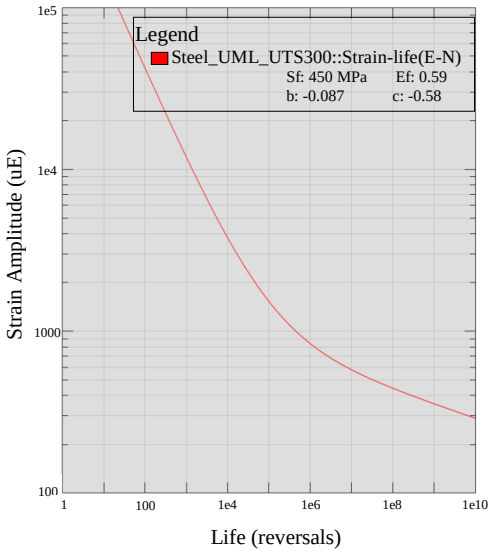

Figure 6: Strain life (Steel UML UTS300).

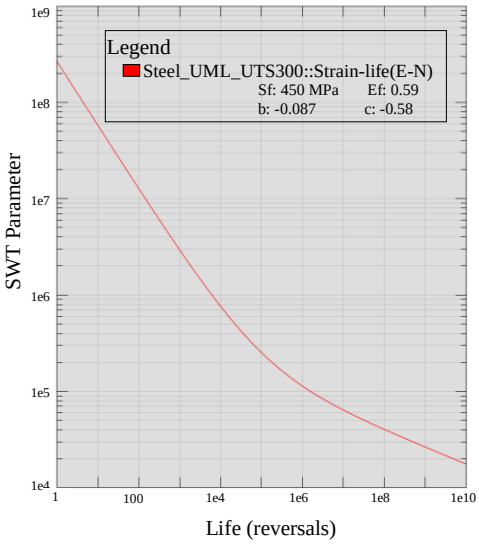

Figure 7: Smith-Watson-Topper (Steel UML UTS300).

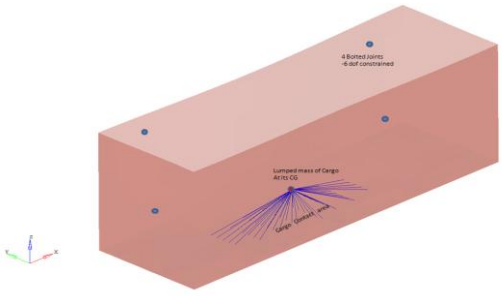

Figure 8: Linear FEA model of the stowage box.

QUASI-STATIC RESTRAINED MASS ASSUMPTION

Due to time and budget constraints, generally linear strength and durability analyses are performed for determining the load carrying capacity of stowage elements. The damage due to the extra impact loads caused by the cargo being thrown up and down on the box floor by the rough terrain is assumed to be negligible and ignored.

For linear FEA, the box is modeled with shell elements and the cargo is modeled as a lumped mass attached to the floor via rigid elements, as shown in Figure 8. At the four bolted attachments all six degrees of freedom (translations and rotations) of the box surface are constrained to the vehicle hull. Linear analysis is used to recover stresses for a unit gravity load applied at the mass center of the cargo. The stress contribution caused by the weight of the box is also included in the total stress.

Within Design Life the acceleration time history is used as quasi-static g-loads (with the mass of the box and cargo) and superimposed with the unit stresses to create elemental stress and strain time histories. Applying these to the fatigue process and the scenario outlined in the last section (loads, duty cycle, and damage accumulation method) gives a damage prediction for the box carrying the maximum rated cargo and is shown in Figure 9. In this case, the maximum accumulated damage of 0.27 occurs at the attachment point (bolt hole) and the associated minimum fatigue life is 3.6 times the duty cycle. Taking into consideration all variations in geometric tolerances, material properties, and driving speed used for calculating the virtual loads, a factor of safety of 1.3 to 1.5 is usually recommended [1]. Hence the box can withstand 2.4 to 2.8 times the duty cycle before the first crack is initiated.

DYNAMIC EXPLICIT FEA

Stress and strain time histories can also be recovered from an explicit finite element model of the stowage box, fabric bag, and sand. This study applies Altair's RADIOSS explicit solver and reuses the stowage box shell element mesh and material properties from the linear model. The

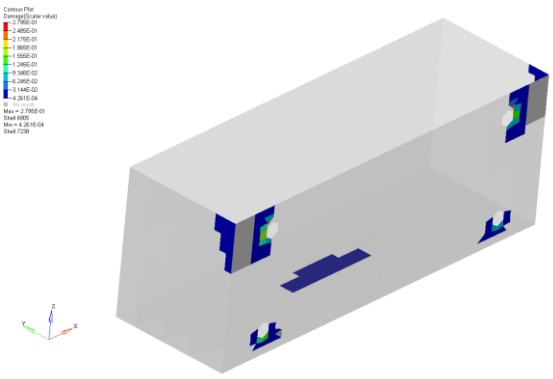

Figure 9: Linear FEA damage result.

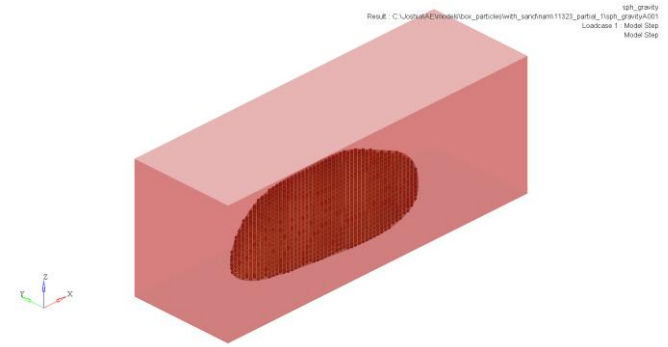

Figure 10: RADIOSS SPH particles.

bag receives a similar shell representation and the fabric is an elastic orthotropic material with the following properties.

Density = 7.225×10^{-7} kg/mm^3
E_{11} =0.45 GPa
E_{22} = 0.45 GPa
Poisson's ratio$_{12}$ = 0.35
Shear modulus (all directions) = 0.1 GPa

The sand is modeled using RADIOSS SPH particles as illustrated in Figure 10. Smooth Particle Hydrodynamics (SPH) Finite Point Method (FPM) is a technique used to analyze bodies that do not have high cohesive forces among themselves and undergo large deformation, such as liquids and gases [3]. It is also common to use SPH elements to represent soil and sand in the analysis of mine blast.

The sand inside the bag is discretized into 7119 SPH elements, each with a mass of 0.0126 kg, totaling 90.1 kg. The following material properties are used to represent the sand.

Density = 1.6×10^{-6} kg/mm^3
Young's modulus = 7.1667×10^{-3} GPa
Poisson's ratio = 0.304 GPa

Two contact interfaces are modeled, the first between the sand and bag and the second between the bag and box. The sand particles are thus allowed to slide inside the bag and against each other.

In a virtual test, the sand bag is dropped from a height of 50 mm onto the floor under the influence of gravity and simulated until large motions damp out. Figures 11 to 14 depict the drop sequence and demonstrate the fluid motion of the sand within the bag. The reaction force between the box and the sand bag is recovered and shown in Figure 15.

In the context of the quasi-static linear solution, this drop scenario is a 1.0 g event and for reference is also shown on Figure 15. It is evident that the impact of a bouncing bag

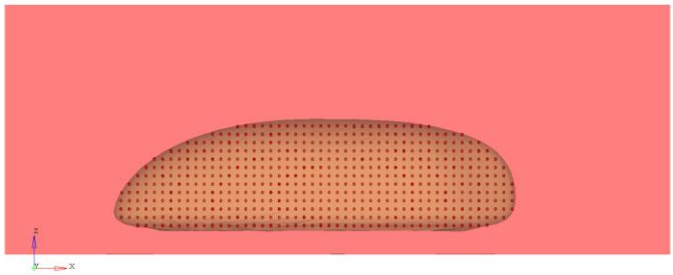

Figure 11: SPH particle model at 0 ms.

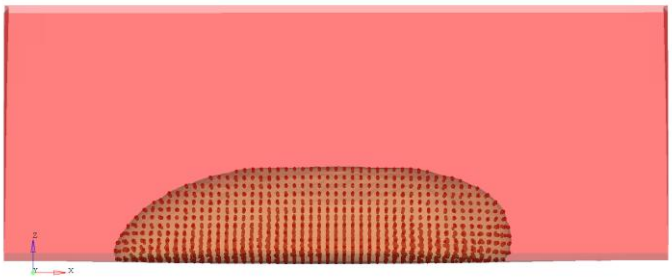

Figure 12: SPH particle model at 200 ms.

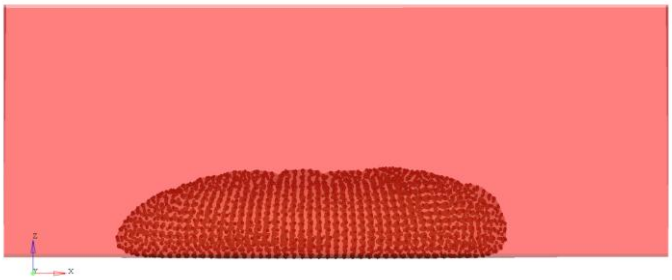

Figure 13: SPH particle model at 500 ms.

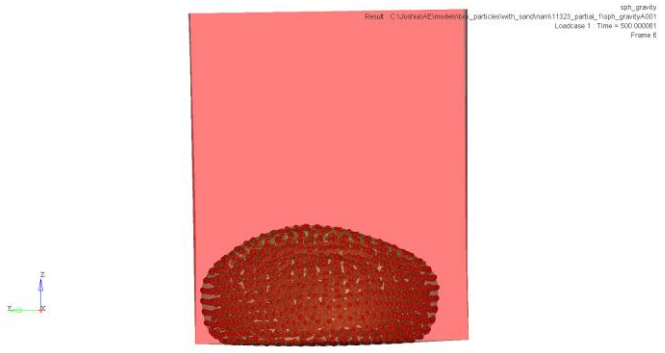

Figure 14: SPH particle model at 200 ms.

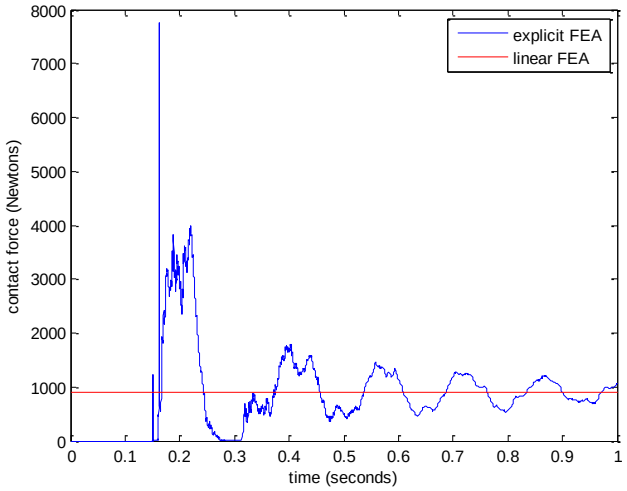

Figure 15: RADIOSS SPH particles.

can have a significant effect on the applied force and should be considered in damage models of such components.

Stress-time histories on the stowage box obtained from this model feed directly into nCode Design Life without the need for superposition. Damage is then computed in exactly the same manner as before. Unfortunately the time and computer resources required to run an entire duty cycle in this way prohibit application to the complete virtual durability process (not to mention design exploration, iteration, optimization, and associated variability and reliability analysis). This limited example utilized an 8 CPU workstation and ran for 2 days to recover stresses and reaction forces over the 1.5 second interval.

REDUCED ORDER MODEL

It is clear from comparison of the quasi-static simulation and results observed in testing that a significant component of the loading response can be missing. The large difference in loads obtained from the quasi-static and explicit simulations motivates further investigation of contact simulation. One approach to generating a tractable numerical solution for the complete time history is to create an approximate model. To this end a particle based contact model is proposed, calibrated to a limited set of data, simulated over the duty cycle, applied to compute damage and ultimately compared to the available quasi-static result.

The Particle Model

The intent of the model is to capture the internal compression and restitution properties of the sand within the bag. At a minimum two particles are required. A vertical sprung/un-sprung mass configuration is used with a linear spring and damper arrangement as shown in Figure 16. No free length of the interconnecting spring is required as only the particle m_2 will be allowed to contact the bottom surface (which is termed a shelf).

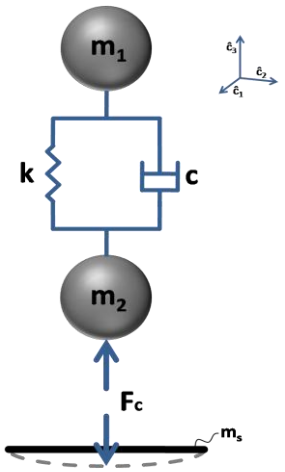

Figure 16: The particle model.

The particle model is connected in the appropriate location on the three dimension rigid body chassis. As stated earlier, the chassis motion (position, orientation, velocity, angular velocity, acceleration, and angular acceleration) is prescribed. To formulate the equations of motion and solve the impact events, the velocity and acceleration of important points are required. Specifically, the un-deformed shelf reference point P and particles m_i (i = 1,2) relative to an inertial point O and associated reference frame are required. Introducing relative coordinates q_i and chassis (ch) fixed base vectors $\hat{c}_i$ (shown in Figure 16) the following relationships are constructed.

$$\vec{v}^{\,P} = \vec{v}^{\,O} + \vec{\omega}^{ch} \times \vec{r}^{\,OP} \tag{1}$$

$$\vec{a}^{\,P} = \vec{a}^{\,O} + \vec{\alpha}^{ch} \times \vec{r}^{\,OP} + \vec{\omega}^{ch} \times (\vec{\omega}^{ch} \times \vec{r}^{\,OP}) \tag{2}$$

$$\vec{r}^{\,Om_i} = \vec{r}^{\,OP} + q_i \hat{c}_3 \tag{3}$$

$$\vec{v}^{\,m_i} = \vec{v}^{\,P} + \dot{q}_i \hat{c}_3 + \vec{\omega}^{ch} \times \vec{r}^{\,Om_i} \tag{4}$$

$$\vec{a}^{\,m_i} = \vec{a}^{\,P} + \ddot{q}_i \hat{c}_3 + \vec{\omega}^{ch} \times \dot{q}_i \hat{c}_3 + \vec{\alpha}^{ch} \times \vec{r}^{\,Om_i} + \vec{\omega}^{ch} \times \vec{v}^{\,m_i} \tag{5}$$

In Equations (1-5) the velocities and accelerations are absolute, referenced relative to the inertial frame fixed in the ground.

The particle m_2 is allowed to impact the surface of the shelf and thus requires an impulsive solution associated with the instantaneous change in velocity of the shelf. The pre and post impact relationship is described using the inelastic coefficient of restitution (CoR = 1) appearing in Equation (6).

$$\left(m_2\bar{v}_{m_2}^- + m_s\bar{v}_{m_s}^- = (m_2 + m_s)\bar{v}_{m_2}^+\right)\cdot\hat{c}_3 \qquad (6)$$

At the instant before impact the velocity of m_2 and m_s can be computed from the known state using (1) and (4). The unit vector $\hat{c}_3$ dot product reduces the vector equation in (6) to a scalar relationship enabling the solution for the coordinate velocity $\dot{q}_2$ at the instant after impact. The value m_s is determined from the actual mass of the bottom plate of the box (12.6 kg) and applying a lumped mass approximation for an assumed uniform velocity distribution (which upon integration yields $\frac{1}{9}$).

The impact events represent infinite forces which when taken directly will result in immediate failure of the structure. However, the impulse occurs with zero deflection such that stresses away from the contact location are negligible. Peak stresses occur some finite time afterwards at seams, stress concentrations, and mounting points when maximum deflection is reached. Such behavior is represented in the model.

The applied forcing elements in the model represent the internal spring and damping characteristics of the sand and the contact interface between the bag and the shelf. These relationships are assumed to be linear and take the form of Equations (7-9), taking care to only apply positive values of the contact damping force.

$$\bar{F}_{contact} = -k_{F_C}q_2\hat{c}_3 - c_{F_C}\dot{q}_2\hat{c}_3 \qquad (7)$$

$$\bar{F}_{spring} = k(q_2 - q_1)\hat{c}_3 \qquad (8)$$

$$\bar{F}_{damper} = c(\dot{q}_2 - \dot{q}_1)\hat{c}_3 \qquad (9)$$

The equations of motion can now be constructed from a trivial application of D'Alembert's Principle which allows one to ignore the constraint forces by projecting an incomplete Newton form along the modes of free motion $\hat{c}_3$. The result is two scalar second order differential equations solvable directly for the unknown $\ddot{q}_i$ instead of six differential equations plus four algebraic constraint equations. These reduced equations account for the full three dimensional motion of the constrained particle system.

$$\left(m_1\bar{a}^{m_1} = m_1\bar{g} + \bar{F}_{damper} + \bar{F}_{spring}\right)\cdot\hat{c}_3 \qquad (10)$$

$$\left(m_C\bar{a}^{m_2} = m_C\bar{g} - \bar{F}_{damper} - \bar{F}_{spring} + \bar{F}_{contact}\right)\cdot\hat{c}_3 \qquad (11)$$

In Equation (11) the mass quantity m_c varies discretely based on the contact condition. During motion above the shelf, m_c is identically m_2 and when in contact ($q_2 < 0$) it assumes the value $m_2 + m_s$. To minimize complexity the shelf is not given its own degree of freedom. This is to say that once contact is terminated the shelf stops moving and "waits" at a chassis relative rest condition for contact to begin again.

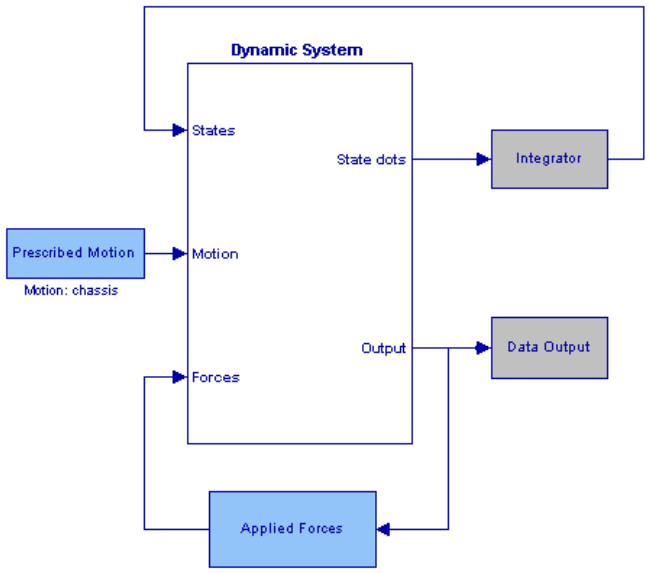

Figure 17: Simulink system model.

Implementation

The particle model was given a MATLAB / Simulink implementation in the form of a system model and reconfigurable environment. Figure 17 shows the modularity of the solution with input prescribed motions, the dynamic system (equations of motion), applied forces, and numerical time integration subsystems. The environment can be quickly reconfigured from an interactive pull-down menu (or the scripts they link to) in order to accept different input profiles and model parameters. Scenarios include varying roads motions and a stationary profile for drop tests as well as parameter variations and a verification suite. All of which may be re-run without altering the underlying Simulink model.

The prescribed motions subsystem acquires the base excitation as a function of the current simulation time. This amounts to reading the imported DADS vehicle motion data (or a stationary input) utilizing a set of linearly interpolated look-up table elements.

The equations of motion subsystem implements internal forces (8) and (9) and solves Equations (10) and (11) for the unknown coordinate accelerations. The model detects the presence of contact and uses the appropriate value of m_c.

The applied forces subsystem encapsulates the forcing interface between the shelf surface and m_2. It evaluates equation (7) and makes data available for output.

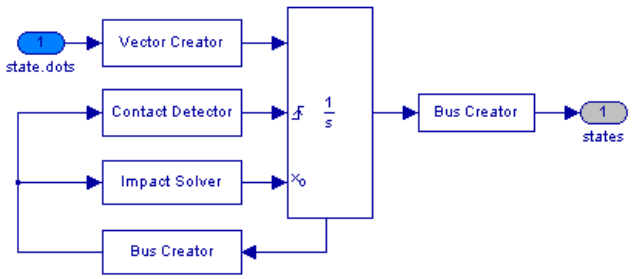

Figure 18: Simulink custom system integrator.

The integrator incorporates the discontinuities of impact solutions as is depicted in Figure 18. The positive to negative zero crossing of the second particle state (q_2) triggers the integrator to reset with the computed inelastic momentum balance of Equation (6) [4].

Parameter Identification

With a simulation environment configured and verified, the model must now be calibrated to reproduce the drop test result obtained from the high fidelity explicit FEA solution (or an equivalent physical test).

Mining the data of the high fidelity model can produce an overwhelming amount of information which one would like to match in the reduced order model. Notable quantities are maximum displacement of the shelf, frequency content of various motions, the CG and mass distribution of the sand, peak loads, and the load time history of the bag-shelf contact. Ultimately the effectiveness of matching the loads and first frequencies shown in Figure 15 is all will matter in applying the result to the virtual durability process.

To reproduce the steady state load, we require that the sum of m_1 and m_2 be equal to 91 kg. It is then natural to introduce the free parameter mass ratio $r = m_2/(m_1+m_2)$. The adjustable parameters are then r, k, c, k_{Fc}, and c_{Fc}.

The maximum displacement from the linear FEA result can be used to obtain a lower bound on the stiffness k_{Fc} (in this case 59 N/mm). This value will need to be several times stiffer to more closely match the frequency response.

Choosing r = 0.99 and k = c = 0, allows rapid one degree of freedom tuning to the dominant frequency and the damping character of the system. Then one may proceed to mixing in the second degree of freedom which allows a nice match on the first impact event, peak and trough amplitudes throughout and approximate frequency.

In the case of the drop test loads shown in Figure 15 the final values of the parameters are:

- r = 0.4
- k = 75,000 N/m
- c = 350 Ns/m
- k_{Fc} = 9x59x10^3 N/m

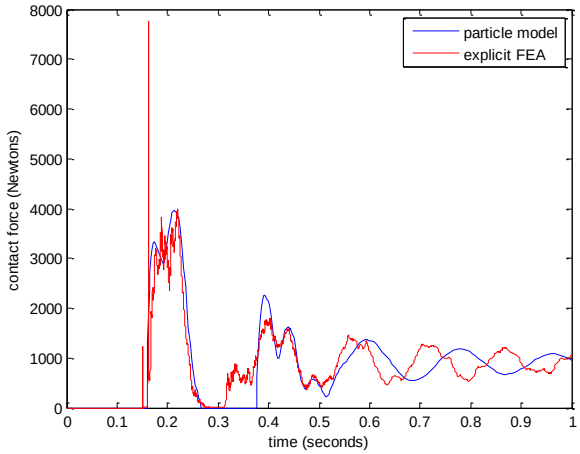

Figure 19: Contact force comparison of high fidelity explicit FEA and simple particle model after parameter identification.

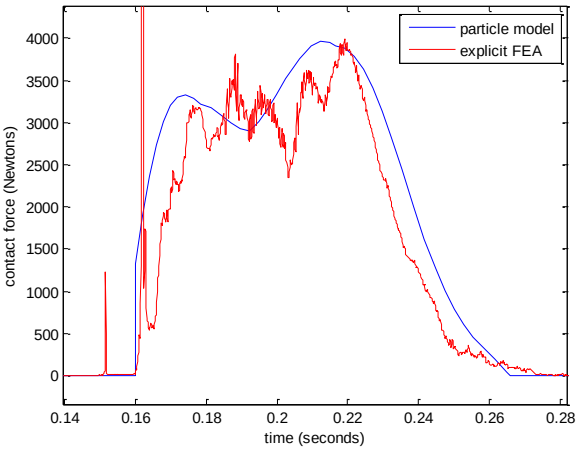

Figure 20: Contact force comparison showing bimodal response.

- c_{Fc} = 2000 Ns/m

The resulting contact force time histories are compared to the original drop test in Figures 19 and 20. For the purposes of structural loads, the highest frequency spikes are not of interest because no appreciable displacement, stress, or strain, is accumulated away from the contact site in the short period of time. These figures demonstrate high quality matching properties. Qualitatively, the bimodal character of the initial impact response is captured nicely (as shown in Figure 20). After the initial impact, both models rebound and bring the contact force to zero throwing the sand bag free only once.

There is however a notable difference in the nature of the second impact event. The high fidelity simulation initiates

contact softly and distributes the load over three oscillations. This is understood to be the result of the dynamic shelf coming up to meet the sand bag above the zero point. The reduced order model does not contain a degree of freedom for the shelf and must wait for contact when the bag crosses zero deflection. This causes the reduced order model to see a second impact more like the first while the high fidelity model does not.

Quantitatively the peak load is consistent with that of the drop test (within 1%) and the first frequency is within 20% during the settling period after the second impact. This matching capability is within the loads variability already present in the durability testing process [1].

Results

The particle model implementation with tuned parameters has been applied to the road excitation problem and compared to the fatigue results obtained from the linear g-load method.

The applied forces from the two methods are compared in Figures 21 and 22. The low amplitude responses are observed to match very closely. During aggressive excitation the payload is observed to separate from the box floor (jump) where the contact force becomes zero for short durations. The subsequent impact results in a significant increase in loads.

The loads from the particle model are then passed on to nCode Design Life and an equivalent fatiue process is performed. In this case, the stowage box FEA model is run quasi-statically with an attached lumped mass (the cargo). Linear stresses are recoved for a unit force applied over the contact area on the box floor. The unit stresses are then superimposed with the load-time histories derived from the particle model to estimate the damage and fatigue life of the stowage box.

The damage is increased by 233% compared to the damage obtained from the g-load time history, as shown in Figure 23. The corresponding life is 1.1 duty cylces. Applying a factor of safety of 1.3 to 1.5, the fatigue life is estimated to be 0.73 to 0.85 times the duty cycle.

CONCLUSION

A method for approximate loose cargo as present in off-road stowage systems has been presented and implemented. The method reduces the behavior or computationally intensive high fidelity explicit FEA simulations to a two degree of freedom particle contact model. The essential character of the high fidelity response is captured to enable simulation over the entire duty cycle as required for incorporation in a virtual durability process. Simulation demonstrates increased loads relative to the traditional quasi-static result and supports a recent test observation where a stowage element has failed.

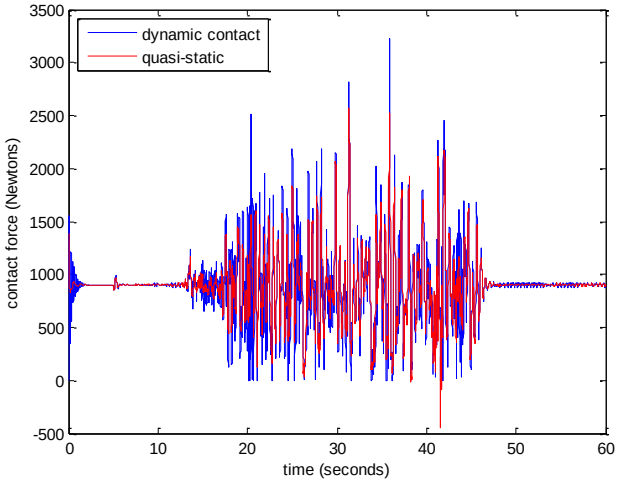

Figure 21: Fatigue loads comparison.

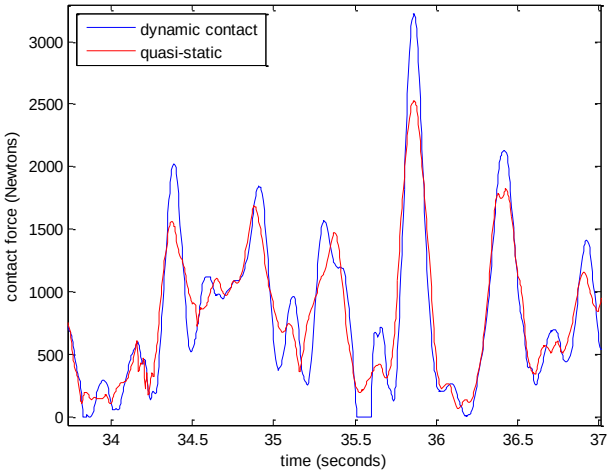

Figure 22: Fatigue loads comparison.

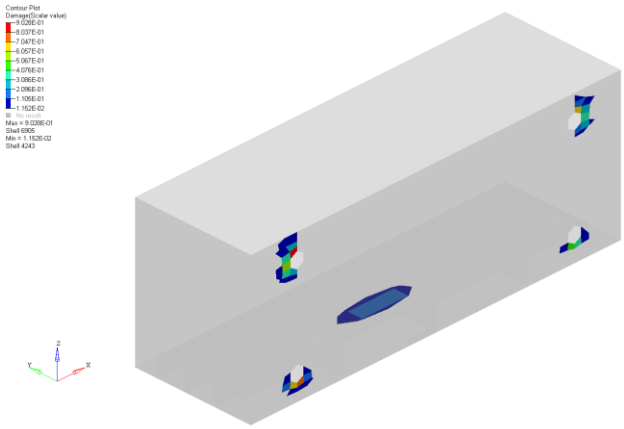

Figure 23: Stowage box damage with loose cargo.

In the specific application to a stowage box, the model demonstrates a 233% increase in damage which reduces the reliable estimate of the overall life from 2.4 to 2.8 down to 0.73 to 0.85 times the duty cycle. Under such circumstances this difference will cause a properly designed part to fail prematurely.

Qualitative inspection of the new loads profile suggests that a similar increase in amplitudes may be obtained from a linear FEA transient solution. The explicit FEA model and its reduced order representation provide a means for such comparison which is a topic for future work.

REFERENCES

[1] N. Purushothaman, P. Jayakumar, J. Critchley, S. Datta, and V. Pisipati, "A Robust Durability Process for Military Ground Vehicles", Proceedings of the 2009 Ground Vehicle Systems Engineering and Technology Symposium (GVSETS), August, 2009.

[2] "Online Manuals 6.0", and "Design Life Theory Guide 6.0", HBM-nCode, 2010, Marlborough, MA, USA, 2010, www.ncode.com.

[3]"RADIOSS/OptiStruct User's Guide", Altair Engineering Inc., Troy, MI, 2010, USA, www.altairhyperworks.com.

[4] MATLAB/Simulink R2008a Documentation, "Bouncing Ball Model: Use of Zero Crossing Detection," The Mathworks, 2008.